Exploring the ages of rotating stars using galactic dynamics: a novel approach to calibrating gyrochronology

Ruth Angus, Angus Beane, Adrian Price-Whelan, Elisabeth Newton, Jennifer van Saders, Jason Curtis, Lauren Anderson, Rocio Kiman, Travis Berger, & Dan Foreman-Mackey

ABSTRACT

The rotational evolution of cool dwarfs is poorly constrained after ∼2-3 billion years due to a lack of precise ages and rotation periods for old main-sequence stars. In this work, we use the velocities of low-mass *Kepler* dwarfs as an age proxy, to reveal their rotational evolution and demonstrate that kinematics could be a useful tool for calibrating gyrochronology. We find that, at young ages, lower-mass stars spin more slowly than higher-mass stars because their stronger magnetic fields lead to more efficient angular momentum loss. This reflects the behavior of young open clusters such as the Pleaides, Praesepe, and the Hyades. However, at older ages we find that late G and early K dwarfs rotate at the same rate as late K dwarfs of the same age, and eventually rotate faster. These results align with recent findings from the rotation periods of stars in middle-aged open clusters and theoretical models that vary the rate of surface-to-core angular momentum transport as a function of time and mass. Finally, we find no evidence for mass-dependent heating in a sample of K and M dwarfs in the *Kepler* field.

1. Introduction

1.1. Gyrochronology

Stars with significant convective envelopes ($\lesssim 1.3\ M_{\odot}$) have strong magnetic fields and spin more slowly over time through magnetic braking (*e.g.* Schatzman 1962; Weber and Davis 1967; Skumanich 1972; Kawaler 1988; Pinsonneault et al. 1989). Although stars are typically born with random rotation periods, ranging from 1 to 10 days, observations of young open clusters reveal that their rotation periods converge onto a unique sequence by ∼500-700 million years (*e.g.* **??**). After this time, the rotation period of a star is thought to be determined, to first order, by its color and age alone. This is the principle behind gyrochronology – the method of inferring a star's age from its rotation period (*e.g.* Barnes 2003, 2007, 2010; Meibom et al. 2011, 2015). However, new photometric rotation periods made available by the *Kepler* (Borucki et al. 2010) and *K2* (Howell et al. 2014) missions (*e.g.* McQuillan et al. 2014; García et al. 2014; Douglas et al. 2017; Rebull et al. 2017; Meibom et al. 2011, 2015; Curtis et al. 2019) reveal that rotational evolution is more complicated than previously thought. For example, the M dwarfs in the $\sim$ 650 Myr Praesepe cluster spin more slowly than the G dwarfs. In theory this is because lower-mass stars have deeper convections zones which generate stronger magnetic fields and more efficient magnetic braking. However, in the 1.1 Gyr NGC 6811 cluster, late-K dwarfs rotate at the *same* rate as early-K dwarfs (Curtis et al. 2019). In other words, convection zone depth cannot be the only variable that affects stellar spin-down rate. New semi-empirical models that vary the rate of angular momentum redistribution in the interiors of stars are able to reproduce this flattened period-color relation (Spada and Lanzafame 2019). These models suggest that mass and age-dependent angular momentum transport between the cores and envelopes of stars has a significant impact on their surface rotation rates. Another example of unexpected rotational evolution is seen in old field stars which appear to rotate more rapidly than classical gyrochronology models predict (Angus et al. 2015; van Saders et al. 2016, 2018; Metcalfe and Egeland 2019). A mass-dependent modification to the classical $P_{\rm rot} \propto t^{\frac{1}{2}}$ spin-down law (Skumanich 1972) is required to reproduce these observations. To fit magnetic braking models to these data, a cessation of magnetic braking is required after stars reach a Rossby number (Ro; the ratio of rotation period to convective turnover time) of around 2 (van Saders et al. 2016, 2018).

The rotational evolution of stars is clearly a complicated process and, to fully calibrate the gyrochronology relations we need a large sample of reliable ages for stars spanning a range of ages and masses. In this paper, we use the velocity dispersions of field stars to qualitatively explore the rotational evolution of GKM dwarfs, and show that kinematics could provide a gyrochronology calibration sample.

1.2. Using kinematics as an age proxy

Stars are thought to be born in the thin disk of the Milky Way (MW), orbiting the galaxy with a low out-of-plane, or vertical, velocity (W, or $v_{\mathbf{z}}$), just like the star-forming molecular gas observed in the disk today (*e.g.* Stark and Brand 1989; Stark and Lee 2005; Aumer and Binney 2009; Martig et al. 2014; Aumer et al. 2016). On average, the vertical velocities of stars increase over time (*e.g.* Nordström et al. 2004; Holmberg et al. 2007, 2009; Aumer and Binney 2009; Casagrande et al. 2011). Although the cause of dynamical heating is not well understood, interactions with giant molecular clouds, spiral arms and the galactic bar are thought to play an important role (see Sellwood 2014, for a review of secular evolution in the MW). Although the velocity of any individual star will only provide a weak age constraint, the velocity *dispersion* of a *group* of stars can indicate whether, on average, that group is old or young relative to other groups. In this work we compare the velocity dispersions of groups of field stars in the Galactic thin disk to ascertain which groups are older and which younger and draw conclusions based on the implied relative ages.

Vertical velocity, $v_{\mathbf{z}}$, can only be calculated with full 6-dimensional position and velocity information, and unfortunately most stars with measured rotation periods do not have radial velocity (RV) measurements because they are relatively faint *Kepler* targets ($\sim$12th-17th magnitudes). For this reason, we used velocity in the direction of galactic latitude, $v_{\mathbf{b}}$, to approximate $v_{\mathbf{z}}$. The *Kepler* field is positioned at low galactic latitude (b=$\sim$5-20°), so $v_{\mathbf{b}}$ is a close (although imperfect – see section 3) approximation to $v_{\mathbf{z}}$. Because we use $v_{\mathbf{b}}$ rather than $v_{\mathbf{z}}$ we cannot calculate absolute kinematic ages using an age-velocity dispersion relation (AVR). However, regardless of direction, velocity dispersion is expected to monotonically increase over time, and can therefore be used to *rank* groups of stars by age.

This paper is laid out as follows: in section 2 we describe our sample selection process and the methods used to calculated stellar velocities. We also establish that $v_{\mathbf{b}}$ velocity dispersion, $\sigma_{v\mathbf{b}}$, can be used as an age proxy by demonstrating that neither mass-dependent heating nor the selection function seems to strongly affect on our sample. In section 3 we use kinematics to investigate the relationship between rotation period, age and color/$T_{\rm eff}$ in the field and interpret our results in section 4.

2. Method

2.1. The data

We used the publicly available *Kepler*-*Gaia* DR2 crossmatched catalog[1] to combine the McQuillan et al. (2014) catalog of stellar rotation periods, measured from *Kepler* light curves, with the *Gaia* DR2 catalog of parallaxes, proper motions and apparent magnitudes. Reddening and extinction from dust was calculated for each star using the Bayestar dust map implemented in the `dustmaps` *Python* package (M. Green 2018), and `astropy` (Astropy Collaboration et al. 2013). We estimated effective temperatures from dereddened *Gaia* $G_{BP}-G_{RP}$ color, using an 8th-order polynomial relation calibrated using .... stars ask Jason for details.

$$\mathrm{T}_{\mathrm{eff}} = 8960 - 4802C + 1931C^2 - 2446C^3 + 2669C^4 - 1324C^5 + 301C^6 - 26C^7, \quad (1)$$

where C is *Gaia* $G_{BP} - G_{RP}$.

Visual binaries and subgiants were removed from the sample by applying cuts to the color-magnitude diagram (CMD), shown in figure 1. A 6th-order polynomial was fit to the main sequence and raised by 0.27 dex to approximate the division between single stars and visual binaries. All stars above this line were removed from the sample. Subgiants were also removed by eliminating stars brighter than 6th magnitude in *Gaia* G-band.

The dwarf stars in the McQuillan et al. (2014) sample are shown on a *Gaia* color-magnitude diagram (CMD) in figure 1. The stars are colored by their gyrochronal age, calculated using the (Angus et al. 2019) gyrochronology relation. The stars with old gyrochronal ages, plotted in yellow hues, predominantly lie along the upper edge of the MS, where stellar evolution models predict old stars to be, however the majority of these 'old' stars are bluer than $G_{BP} - G_{RP} \sim 1.5$ dex. This suggests that either old M dwarfs are missing from the McQuillan et al. (2014) catalog, or the Angus et al. (2019) gyrochronology relation under-predicts the ages of low-mass stars. Given that lower-mass stars stay active for longer than higher-mass stars (*e.g.* West et al. 2011), and are therefore more likely to have measurable rotation periods at old ages, the latter scenario seems more likely.

The `Pyia` (Price-Whelan 2018) and `astropy` (Astropy Collaboration et al. 2013; Price-Whelan et al. 2018) *Python* packages were used to calculate stellar velocities. `Pyia` calculates velocity samples from the full *Gaia* uncertainty covariance matrix via Monte Carlo sampling. It therefore not only incorporates uncertainties on the *Gaia* positions parallaxes and proper

[1]Available at gaia-kepler.fun

Fig. 1.— Dereddened MS *Kepler* stars with McQuillan et al. (2014) rotation periods on the *Gaia* CMD. We excluded visual binaries by removing stars above the dashed line. Points are colored by their gyrochronal age, according to the Angus et al. (2019) gyrochronology relation. A general age gradient is visible across the main sequence.

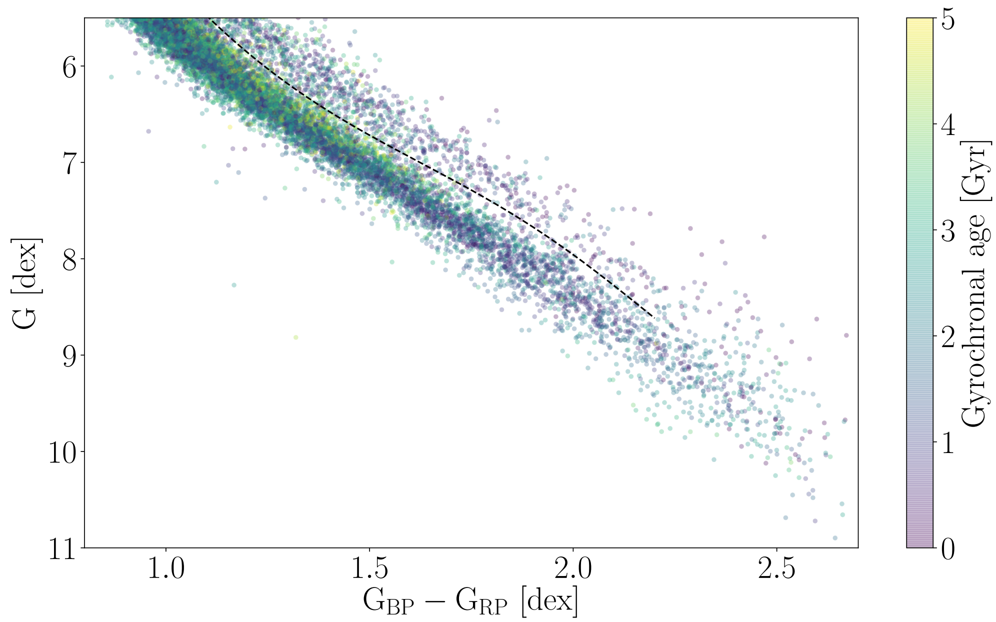

motions, it also accounts for the *covariance* between these properties. Stars with negative parallaxes, parallax signal-to-noise ratios less than 10, stars fainter than 16th magnitude, stars with absolute $v_{\mathbf{b}}$ uncertainties greater than 1 kms^{-1} and stars with galactic latitudes greater than 15° (justification provided below) were removed from the sample.

2.2. Validating $v_{\mathbf{b}}$ dispersion as an age proxy

There are two main reasons why $v_{\mathbf{b}}$ velocity dispersion may not be a good age proxy. Firstly, mass-dependent heating may act on the sample, meaning that velocity dispersion depends on both age and mass, so cannot be interpreted as a simple age proxy. Secondly, since stars in the *Kepler* field have a range of galactic latitudes, using $v_{\mathbf{b}}$ as a stand-in for $v_{\mathbf{z}}$ may not be equally valid for all stars, introducing a velocity bias for high latitude stars (which are more likely to be cooler and older). In this section we demonstrate that neither of these problems seem to be a significant issue for our data.

If lower-mass stars experience greater velocity changes when gravitationally perturbed and are dynamically heated more efficiently than higher-mass stars, velocity dispersion would be a function of *both* age and mass and cannot be straightforwardly interpreted as an age proxy. So, in order to establish whether $\sigma_{v\mathbf{b}}$ can be used as an age proxy, we searched for signs of mass-dependent heating within the *Kepler* field. Mass-dependent dynamical heating has not been unambiguously observed in the galactic disk because of the strong anti-correlation between stellar mass and stellar age. Less massive stars do indeed have larger velocity dispersions, however they are also older on average. This mass-age degeneracy is highly reduced in M dwarfs because their main-sequence lifetimes are longer than the age of the Universe, however no evidence for mass-dependent heating has been found in M dwarfs (*e.g.* Faherty et al. 2009; Newton et al. 2016).

To investigate whether mass-dependent heating could be acting on the *Kepler* sample, we selected late K and M dwarfs observed by both *Kepler* and *Gaia*, whose MS lifetimes exceed around 11 Gyrs and are therefore representative of the initial mass function. We could not perform this analysis on the McQuillan et al. (2014) sample, because only stars with *detectable* rotation periods are included in it and since lower-mass stars stay active for longer it is likely that the oldest stars in this sample have low masses. We selected all *Kepler* targets with dereddened *Gaia* $G_{BP} - G_{RP}$ colors greater than 1.2 (corresponding to an effective temperature $\lesssim$ 4800 K) and absolute *Gaia* G-band magnitudes < 4. We also eliminated visual binaries by removing stars above a 6th order polynomial, fit to the MS on the *Gaia* CMD (similar to the one shown in figure 1). We then applied the quality cuts described above in section 2.1. To search for evidence of mass-dependent heating we calculated the ($v_{\mathbf{b}}$) velocity dispersion of stars in effective temperature bins. Sigma clipping was performed at the 3σ level to remove high velocity outliers before calculating the standard deviation of stars in each bin. These high velocity outliers may be very old late K and M dwarfs, or they result from using $v_{\mathbf{b}}$ instead of $v_{\mathbf{z}}$, which introduces additional velocity scatter.

Figure 3 shows velocity and velocity dispersion as a function of effective temperature [2] for the K and M *Kepler* dwarf sample. Velocity dispersion very slightly *decreases* with decreasing temperature, the opposite of the trend expected for mass-dependent heating, however the slope is only inconsistent with zero at the 1.3 σ level. This trend may be due to a selection bias: cooler stars are fainter and therefore typically closer, with smaller heights above the galactic plane and smaller velocities. The essential point however, is that we do not see evidence for mass-dependent heating acting on stars in the *Kepler* field, indicating that $\sigma_{v\mathbf{b}}$ *can* be used as an age proxy. We also examined the *vertical* velocities of the 537 stars in this sample with RV measurements. Again, we found no evidence for mass-dependent heating: the slope of the velocity dispersion-temperature relation was consistent with zero.

At a galactic latitude of zero, $v_b = v_z$, however for increasing values of b, this equivalence becomes an approximation that grows noisier with b. To test the validity of the $v_{\mathbf{b}} \sim v_{\mathbf{z}}$ approximation over a range of latitudes we downloaded stellar data from the *Gaia* Universe Model Snapshot (GUMS) simulation – a simulated *Gaia* catalog (Robin et al. 2012). We downloaded stars from four pointings in the *Kepler* field with galactic latitudes of around 5°, 10°, 15°, and 20°, out to a limiting magnitude of 16 dex. We found that $v_{\mathbf{b}}$ is drawn from a heavy-tailed distribution, centered on $v_{\mathbf{z}}$, with a standard deviation (calculated as $1.5 \times$ the median absolute deviation) that increased with increasing b. Figure 2 shows how $v_{\mathbf{z}}$ transforms to $v_{\mathbf{b}}$ over a range of Galactic latitudes. The standard deviation of $v_{\mathbf{z}}$-$v_{\mathbf{b}}$ was around 3kms^{-1} at $b \sim 5°$, 4kms^{-}1 at 10°, 6kms^{-}1 at 15°, and 9kms^{-}1 at 20°. Since we are concerned with velocity *dispersions*, rather than velocities themselves, we also compared the $v_{\mathbf{b}}$ and $v_{\mathbf{z}}$ velocity *dispersions* for stars downloaded from the GUMS simulation. For stars at galactic latitudes of 15° or less, $\sigma_{v\mathbf{b}}$ was consistent with $\sigma_{v\mathbf{z}}$, within uncertainties, however, at higher latitudes the two quantities became significantly different. For this reason we proceeded by only including stars with galactic latitudes less than 15° in our analysis. Although it seems that the transformation between $v_{\mathbf{z}}$ and $v_{\mathbf{b}}$ does not *strongly* affect our results, we cannot rule out the possibility that it introduces systematic biases into the velocity dispersions we present here. In *Gaia* DR3, RVs will be available for most stars in this sample, providing an opportunity to validate (or correct) the results presented here.

---

[2]calculated by transforming dereddened *Gaia* colors using equation 1.

To explore the relationship between rotation period, $T_{\rm eff}$ and age, we removed high and low velocity outliers from the McQuillan et al. (2014) sample by performing 3σ sigma-clipping on the $v_{\mathbf{b}}$ velocities. Without sigma-clipping, we found that a small number of high velocity outliers at the low-temperature end of our sample substantially raised the velocity dispersion for cooler stars, however the overall trends remained the same. We also limited the sample to temperatures in the range 5500 K $< T_{\rm eff} <$ 3500 K to avoid biases caused by the selection function at the faint, cool end, and binarity or weakened braking (van Saders et al. 2016) at the hot end.

In this paper, we do not attempt to convert velocity dispersion ($\sigma_{v\mathbf{b}}$) into an age via an age-velocity dispersion relation (AVR) (*e.g.* Holmberg et al. 2009). Although it seems $\sigma_{v\mathbf{b}}$ can be used to roughly rank stars by age, a more careful analysis will be needed to calculate absolute ages. For example, the velocity distributions could be modeled as a mixture of Gaussians in order to account for the additional velocity dispersion caused by the $v_{\mathbf{z}}$-$v_{\mathbf{b}}$ transformation. The RVs of most of these stars will become available in *Gaia* DR3, allowing calculations of $v_{\mathbf{z}}$, which can be used to calculate more reliable ages via an AVR.

Fig. 2.— This figure demonstrates the relationship between $v_{\mathbf{b}}$ and $v_{\mathbf{z}}$ for stars in the *Kepler* field, based on the GUMS simulation. The panels show a kernel density estimator (KDE) (black solid line) for the $v_{\mathbf{z}}$-$v_{\mathbf{b}}$ residuals of stars in the GUMS simulation at four different Galactic latitudes. Blue dashed lines show Gaussian fits to these KDEs. The distributions are close to Gaussians, but with slightly heavy tails. The standard deviations of the Gaussian fits increase with Galactic latitude. This figure illustrates the fact using $v_{\mathbf{b}}$ instead of $v_{\mathbf{z}}$ artificially increases the velocity dispersion, especially at high latitudes.

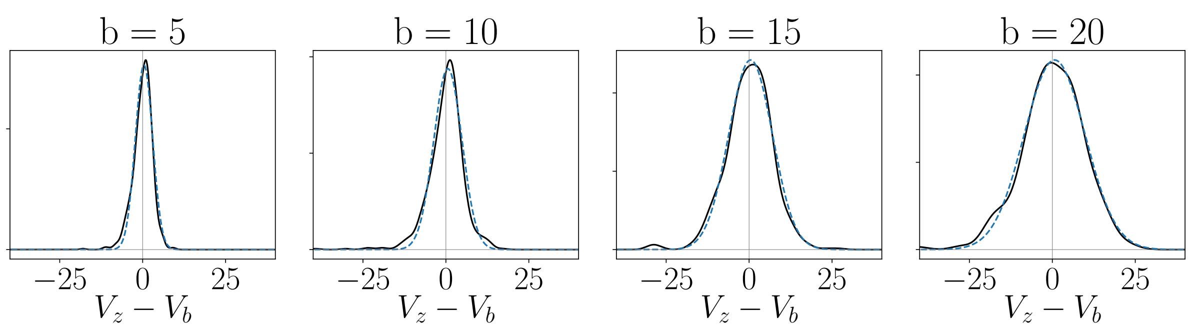

Fig. 3.— Top: Stellar velocity ($v_{\mathbf{b}}$) as a function of $T_{\rm eff}$ for *Kepler* K and M dwarfs. Vertical lines indicate different $T_{\rm eff}$-groupings used to calculate velocity dispersion. Pink stars were not included in velocity dispersion calculations as they were either removed as outliers during a sigma clipping process, or they lie at the sparcely populated, extremely cool end of the temperature range. Velocity dispersion and $T_{\rm eff}$ are slightly positively correlated, likely due to a brightness-related selection bias, indicating that mass-dependent heating does not significantly affect low-mass stars in the *Kepler* field.

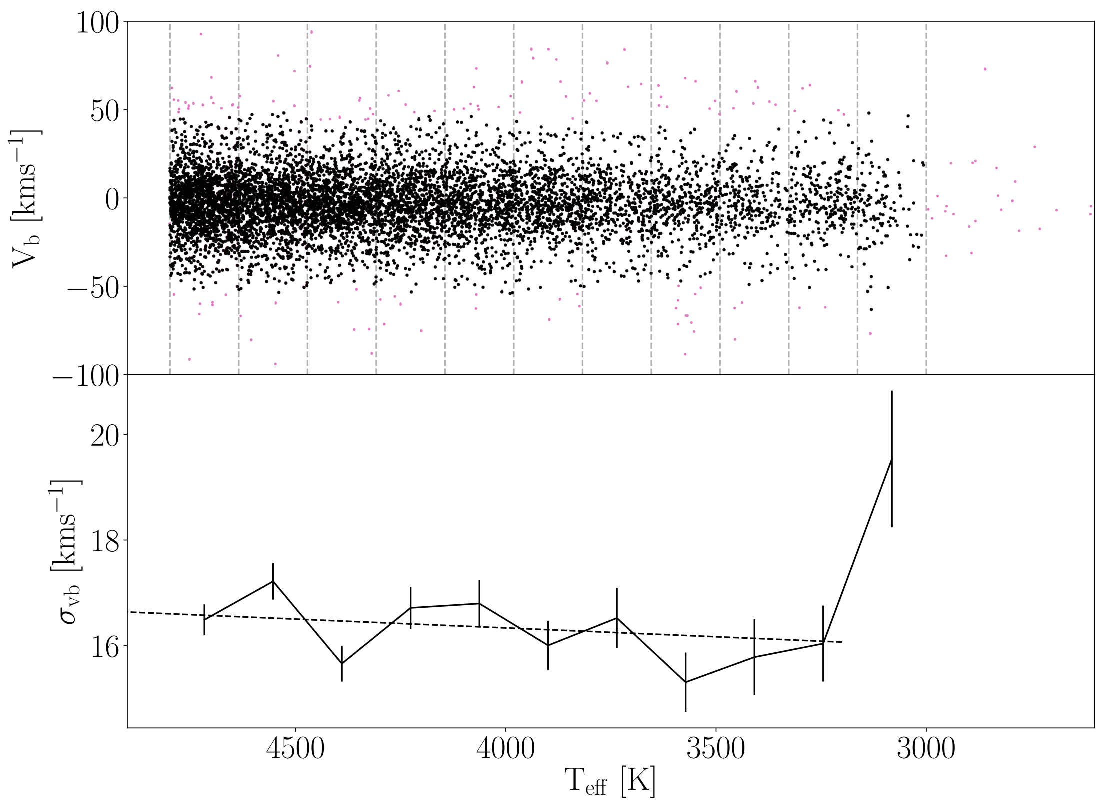

3. Results

3.1. The period-$T_{\rm eff}$ relations, revealed

Figure 4 shows rotation period versus effective temperature for the McQuillan et al. (2014) sample, coloured by the standard deviation of their ($v_{\mathbf{b}}$) velocities, where $\sigma_{v\mathbf{b}}$ was calculated for groups of stars over a grid in $\log_{10}$(period) and temperature. If we assume that mass dependent heating does not strongly affect this sample and $v_{\mathbf{b}}$ at low galactic latitudes is an unbiased tracer of $v_{\mathbf{z}}$, then $v_{\mathbf{b}}$ velocity dispersion can be interpreted as an age proxy and stars plotted in a similar color in figure 4 are similar ages.

Overall, figure 4 shows that velocity dispersion increases with gyrochronal age across all temperatures, implying that both velocity dispersion and rotation period increases with age as expected. Lines of constant age (isochrones) appear to follow the shape of the Praesepe-based gyrochronology model (black dotted line) at young ages. However, at older ages it appears that the relation between rotation period and $T_{\rm eff}$ flattens out, until eventually rotation period *decreases* with decreasing effective temperature at a given age.

Figure 5 shows the same as figure 4, however mass is plotted on the x-axis instead of temperature and the models are those of Spada and Lanzafame (2019). The masses of these stars are taken from the *Kepler* input catalog (**?**). The Spada and Lanzafame (2019) models appear to qualitatively agree with the data: their rotation period-$T_{\rm eff}$ relation flattens out over time and eventually inverts over a narrow range of temperatures. The models reproduce the 'dip' feature seen in the data.

Fig. 4.— Top: Rotation period vs effective temperature for stars in the McQuillan et al. (2014) sample, colored by the velocity dispersions of stars calculated over a grid in $\log_{10}$(period) and $T_{\rm eff}$. Bottom: the velocity dispersions of groups of stars, shown as a solid grid for clarity. The hatched area indicates the temperature regime where selection biases could play an important role, so these velocity dispersions should be interpreted with caution. The black solid lines on both panels show a 1.1 Gyr isochrone, calculated with the Angus et al. (2019) gyrochronology relation, which roughly traces the rotation period gap. The black dashed lines show a 650 Myr isochrone, indicating the location and shape of the Praesepe cluster (to which this gyrochronology model was calibrated). The black points show the 1.1 Gyr NGC 6811 open cluster.

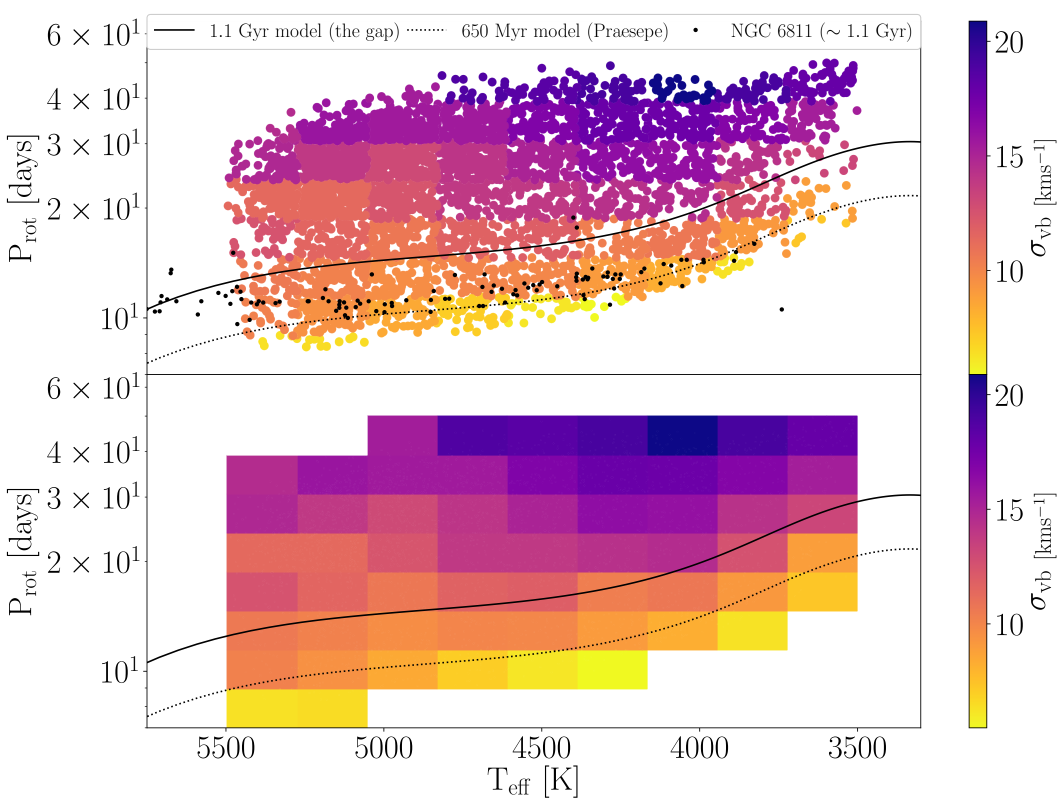

Fig. 5.— Similar to figure 4, with mass instead of $T_{\rm eff}$ on the x-axis. Masses are from the *Kepler* input catalog. The white lines show the Spada and Lanzafame (2019) rotational evolution models at 0.5, 1, 1.5, 2, 2.5, 4 and 4.57 Gyr, where age increases with rotation period. These models include age and mass-dependent coupling between the stellar core and envelope. The oldest models (4 and 4.57 Gyrs), at the largest rotation periods, show an inversion at ∼0.7-0.5 $M_\odot$, where rotation period briefly decreases with decreasing mass. A similar phenomenon is visible in the velocity dispersions of field stars shown as colored points in the background of this figure.

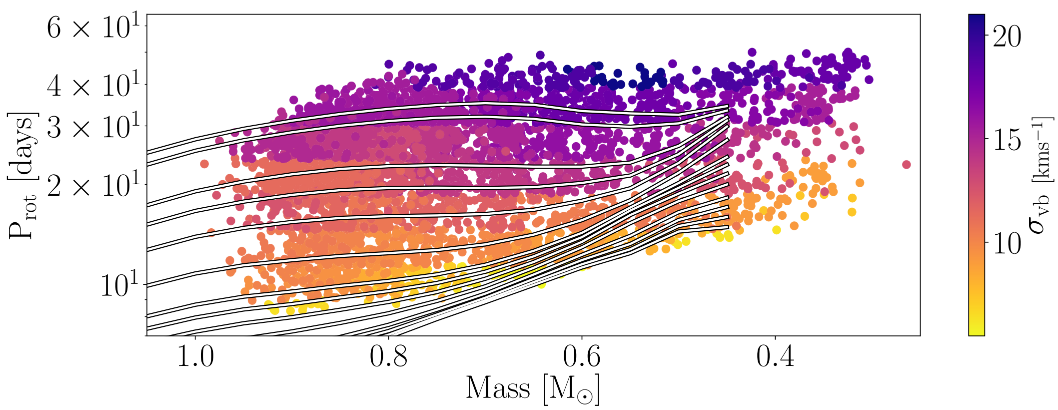

4. Discussion

The results presented above indicate that stars of spectral type ranging from late G to late K follow a braking law that changes over time. In particular, the relationship between rotation period and effective temperature appears to flatten out and eventually invert. These results provide further evidence for ‘stalled’ rotational evolution of K dwarfs, like that observed in open clusters (Curtis et al. 2019) and reproduced by models that vary angular momentum transport between stellar core and envelope with time and mass (Spada and Lanzafame 2019).

The velocity dispersions of stars in the McQuillan et al. (2014) sample provide the following picture of rotational evolution. At young ages, stellar rotation period decreases with mass, likely because lower-mass stars with deeper convection zones have stronger magnetic fields, larger Alfvén radii and therefore experience greater angular momentum loss rate. According to the Spada and Lanzafame (2019) models, there is minimal transportation of angular momentum from the surface to the core of the star at these young ages, so the surface slows down but the core keeps spinning rapidly. At intermediate ages, rotation period is constant with mass, and at late ages rotation period *increases* with mass for GK dwarfs. The explanation for this, according to the Spada and Lanzafame (2019) models, is that lower-mass stars are still braking more efficiently at these intermediate and old ages but their cores are more tightly coupled to their envelopes, allowing angular momentum transport between the two interior layers. Angular momentum resurfaces and prevents the stellar envelopes from spinning-down rapidly.

5. Conclusion

We examined the rotational evolution of *Kepler* field stars using their velocity dispersions as a proxy for age. We found that old groups of cool dwarfs selected to be coeval using the Angus et al. (2019) gyrochronology relation do *not* have the same velocity dispersion across all temperatures. This implies that the Angus et al. (2019) relation, which is based on the period-color relation of the 650 Myr Praesepe cluster, does not correctly describe the period-age-color/$T_{\rm eff}$ relation for old stars. It appears that the period-color/$T_{\rm eff}$ relation changes shape over time in a way that qualitatively agrees with theoretical that which include a mass-dependent core-envelope angular momentum transport (Spada and Lanzafame 2019). At young ages, rotation period is anti-correlated with $T_{\rm eff}$: cooler stars spin more slowly than hotter stars of the same age. However, at intermediate ages the relation flattens out and K dwarfs rotate at the same rate, regardless of mass. At old ages, it seems that cooler K dwarfs spin more rapidly than hotter K dwarfs of the same age. We speculate that the rotation period gap (McQuillan et al. 2014) may separate a young regime where stellar rotation periods decrease with increasing mass from an old regime where periods increase with increasing mass, however more data are needed to provide a conclusive result. Finally, when velocity dispersion is interpreted as an age proxy, it appears that the oldest stars in the McQuillan et al. (2014) catalog are cooler than 4500 K, which suggests that lower-mass stars remain active for longer, allowing their rotation periods to be measured at older ages.

This work was partly developed at the 2019 KITP conference 'Better stars, better planets'. Parts of this project are based on ideas explored at the Gaia sprints at the Flatiron Institute in New York City, 2016 and MPIA, Heidelberg, 2017.

This work made use of the gaia-kepler.fun crossmatch database created by Megan Bedell.

Some of the data presented in this paper were obtained from the Mikulski Archive for Space Telescopes (MAST). STScI is operated by the Association of Universities for Research in Astronomy, Inc., under NASA contract NAS5-26555. Support for MAST for non-HST data is provided by the NASA Office of Space Science via grant NNX09AF08G and by other grants and contracts. This paper includes data collected by the Kepler mission. Funding for the *Kepler* mission is provided by the NASA Science Mission directorate.

This work has made use of data from the European Space Agency (ESA) mission *Gaia* (`https://www.cosmos.esa.int/gaia`), processed by the *Gaia* Data Processing and Analysis Consortium (DPAC, `https://www.cosmos.esa.int/web/gaia/dpac/consortium`). Funding for the DPAC has been provided by national institutions, in particular the institutions participating in the *Gaia* Multilateral Agreement.

REFERENCES

R. Angus, S. Aigrain, D. Foreman-Mackey, and A. McQuillan. Calibrating gyrochronology using Kepler asteroseismic targets. *MNRAS*, 450:1787–1798, June 2015. doi: 10.1093/mnras/stv423.

Ruth Angus et al. Towards precise stellar ages: combining isochrone fitting with empirical gyrochronology. *AJ*, 2019.

Astropy Collaboration, T. P. Robitaille, E. J. Tollerud, P. Greenfield, M. Droettboom, E. Bray, T. Aldcroft, M. Davis, A. Ginsburg, A. M. Price-Whelan, W. E. Kerzendorf, A. Conley, N. Crighton, K. Barbary, D. Muna, H. Ferguson, F. Grollier, M. M. Parikh, P. H. Nair, H. M. Unther, C. Deil, J. Woillez, S. Conseil, R. Kramer, J. E. H. Turner, L. Singer, R. Fox, B. A. Weaver, V. Zabalza, Z. I. Edwards, K. Azalee Bostroem, D. J. Burke, A. R. Casey, S. M. Crawford, N. Dencheva, J. Ely, T. Jenness, K. Labrie, P. L. Lim, F. Pierfederici, A. Pontzen, A. Ptak, B. Refsdal, M. Servillat, and O. Streicher. Astropy: A community Python package for astronomy. *A&A*, 558:A33, October 2013. doi: 10.1051/0004-6361/201322068.

M. Aumer and J. J. Binney. Kinematics and history of the solar neighbourhood revisited. *MNRAS*, 397:1286–1301, August 2009. doi: 10.1111/j.1365-2966.2009.15053.x.

Michael Aumer, James Binney, and Ralph Schönrich. Age-velocity dispersion relations and heating histories in disc galaxies. *MNRAS*, 462(2):1697–1713, Oct 2016. doi: 10.1093/mnras/stw1639.

S. A. Barnes. On the Rotational Evolution of Solar- and Late-Type Stars, Its Magnetic Origins, and the Possibility of Stellar Gyrochronology. *ApJ*, 586:464–479, March 2003. doi: 10.1086/367639.

S. A. Barnes. Ages for Illustrative Field Stars Using Gyrochronology: Viability, Limitations, and Errors. *ApJ*, 669:1167–1189, November 2007. doi: 10.1086/519295.

S. A. Barnes. A Simple Nonlinear Model for the Rotation of Main-sequence Cool Stars. I. Introduction, Implications for Gyrochronology, and Color-Period Diagrams. *ApJ*, 722:222–234, October 2010. doi: 10.1088/0004-637X/722/1/222.

William J. Borucki, David Koch, Gibor Basri, Natalie Batalha, Timothy Brown, Douglas Caldwell, John Caldwell, Jørgen Christensen-Dalsgaard, William D. Cochran, Edna DeVore, Edward W. Dunham, Andrea K. Dupree, Thomas N. Gautier, John C. Geary, Ronald Gilliland, Alan Gould, Steve B. Howell, Jon M. Jenkins, Yoji Kondo, David W. Latham, Geoffrey W. Marcy, Søren Meibom, Hans Kjeldsen, Jack J. Lissauer, David G. Monet, David Morrison, Dimitar Sasselov, Jill Tarter, Alan Boss, Don Brownlee, Toby Owen, Derek Buzasi, David Charbonneau, Laurance Doyle, Jonathan Fortney, Eric B. Ford, Matthew J. Holman, Sara Seager, Jason H. Steffen, William F. Welsh, Jason Rowe, Howard Anderson, Lars Buchhave, David Ciardi, Lucianne Walkowicz, William Sherry, Elliott Horch, Howard Isaacson, Mark E. Everett, Debra Fischer, Guillermo Torres, John Asher Johnson, Michael Endl, Phillip MacQueen, Stephen T. Bryson, Jessie Dotson, Michael Haas, Jeffrey Kolodziejczak, Jeffrey Van Cleve, Hema Chandrasekaran, Joseph D. Twicken, Elisa V. Quintana, Bruce D. Clarke, Christopher Allen, Jie Li, Haley Wu, Peter Tenenbaum, Ekaterina Verner, Frederick Bruhweiler, Jason Barnes, and Andrej Prsa. Kepler Planet-Detection Mission: Introduction and First Results. *Science*, 327(5968):977, Feb 2010. doi: 10.1126/science.1185402.

L. Casagrande, R. Schönrich, M. Asplund, S. Cassisi, I. Ramírez, J. Meléndez, T. Bensby, and S. Feltzing. New constraints on the chemical evolution of the solar neighbourhood and Galactic disc(s). Improved astrophysical parameters for the Geneva-Copenhagen Survey. *A&A*, 530:A138, Jun 2011. doi: 10.1051/0004-6361/201016276.

J. L. Curtis, M. A. Agüeros, S. T. Douglas, and S. Meibom. A Temporary Epoch of Stalled Spin-Down for Low-Mass Stars: Insights from NGC 6811 with Gaia and Kepler. *arXiv e-prints*, May 2019.

S. T. Douglas, M. A. Agüeros, K. R. Covey, and A. Kraus. Poking the Beehive from Space: K2 Rotation Periods for Praesepe. *ApJ*, 842:83, June 2017. doi: 10.3847/1538-4357/aa6e52.

Jacqueline K. Faherty, Adam J. Burgasser, Kelle L. Cruz, Michael M. Shara, Frederick M. Walter, and Christopher R. Gelino. The Brown Dwarf Kinematics Project I. Proper Motions and Tangential Velocities for a Large Sample of Late-Type M, L, and T Dwarfs. *AJ*, 137(1):1–18, Jan 2009. doi: 10.1088/0004-6256/137/1/1.

R. A. García, T. Ceillier, D. Salabert, S. Mathur, J. L. van Saders, M. Pinsonneault, J. Ballot, P. G. Beck, S. Bloemen, T. L. Campante, G. R. Davies, Jr. do Nascimento, J. D., S. Mathis, T. S. Metcalfe, M. B. Nielsen, J. C. Suárez, W. J. Chaplin, A. Jiménez, and C. Karoff. Rotation and magnetism of Kepler pulsating solar-like stars. Towards asteroseismically calibrated age-rotation relations. *A&A*, 572:A34, Dec 2014. doi: 10.1051/0004-6361/201423888.

J. Holmberg, B. Nordström, and J. Andersen. The Geneva-Copenhagen survey of the Solar neighbourhood II. New uvby calibrations and rediscussion of stellar ages, the G dwarf problem, age-metallicity diagram, and heating mechanisms of the disk. *A&A*, 475: 519–537, November 2007. doi: 10.1051/0004-6361:20077221.

J. Holmberg, B. Nordström, and J. Andersen. The Geneva-Copenhagen survey of the solar neighbourhood. III. Improved distances, ages, and kinematics. *A&A*, 501:941–947, July 2009. doi: 10.1051/0004-6361/200811191.

Steve B. Howell, Charlie Sobeck, Michael Haas, Martin Still, Thomas Barclay, Fergal Mullally, John Troeltzsch, Suzanne Aigrain, Stephen T. Bryson, Doug Caldwell, William J. Chaplin, William D. Cochran, Daniel Huber, Geoffrey W. Marcy, Andrea Miglio, Joan R. Najita, Marcie Smith, J. D. Twicken, and Jonathan J. Fortney. The K2 Mission: Characterization and Early Results. *PASP*, 126(938):398, Apr 2014. doi: 10.1086/676406.

S. D. Kawaler. Angular momentum loss in low-mass stars. *ApJ*, 333:236–247, October 1988. doi: 10.1086/166740.

Gregory M. Green. dustmaps: A Python interface for maps of interstellar dust. *The Journal of Open Source Software*, 3(26):695, Jun 2018. doi: 10.21105/joss.00695.

Marie Martig, Ivan Minchev, and Chris Flynn. Dissecting simulated disc galaxies - II. The age-velocity relation. *MNRAS*, 443(3):2452–2462, Sep 2014. doi: 10.1093/mnras/stu1322.

A. McQuillan, T. Mazeh, and S. Aigrain. Rotation Periods of 34,030 Kepler Main-sequence Stars: The Full Autocorrelation Sample. *ApJS*, 211:24, April 2014. doi: 10.1088/0067-0049/211/2/24.

S. Meibom, S. A. Barnes, D. W. Latham, N. Batalha, W. J. Borucki, D. G. Koch, G. Basri, L. M. Walkowicz, K. A. Janes, J. Jenkins, J. Van Cleve, M. R. Haas, S. T. Bryson, A. K. Dupree, G. Furesz, A. H. Szentgyorgyi, L. A. Buchhave, B. D. Clarke, J. D. Twicken, and E. V. Quintana. The Kepler Cluster Study: Stellar Rotation in NGC 6811. *ApJ*, 733:L9, May 2011. doi: 10.1088/2041-8205/733/1/L9.

S. Meibom, S. A. Barnes, I. Platais, R. L. Gilliland, D. W. Latham, and R. D. Mathieu. A spin-down clock for cool stars from observations of a 2.5-billion-year-old cluster. *Nature*, 517:589–591, January 2015. doi: 10.1038/nature14118.

Travis S. Metcalfe and Ricky Egeland. Understanding the Limitations of Gyrochronology for Old Field Stars. *ApJ*, 871(1):39, Jan 2019. doi: 10.3847/1538-4357/aaf575.

Elisabeth R. Newton, Jonathan Irwin, David Charbonneau, Zachory K. Berta-Thompson, Jason A. Dittmann, and Andrew A. West. The Rotation and Galactic Kinematics of Mid M Dwarfs in the Solar Neighborhood. *ApJ*, 821(2):93, Apr 2016. doi: 10.3847/0004-637X/821/2/93.

B. Nordström, M. Mayor, J. Andersen, J. Holmberg, F. Pont, B. R. Jørgensen, E. H. Olsen, S. Udry, and N. Mowlavi. The Geneva-Copenhagen survey of the Solar neighbourhood. Ages, metallicities, and kinematic properties of 14 000 F and G dwarfs. *A&A*, 418:989–1019, May 2004. doi: 10.1051/0004-6361:20035959.

M. H. Pinsonneault, S. D. Kawaler, S. Sofia, and P. Demarque. Evolutionary models of the rotating sun. *ApJ*, 338:424–452, March 1989. doi: 10.1086/167210.

A. M. Price-Whelan, B. M. Sipőcz, H. M. Günther, P. L. Lim, S. M. Crawford, S. Conseil, D. L. Shupe, M. W. Craig, N. Dencheva, A. Ginsburg, J. T. VanderPlas, L. D. Bradley, D. Pérez-Suárez, M. de Val-Borro, (Primary Paper Contributors, T. L. Aldcroft, K. L. Cruz, T. P. Robitaille, E. J. Tollerud, (Astropy Coordination Committee, C. Ardelean, T. Babej, Y. P. Bach, M. Bachetti, A. V. Bakanov, S. P. Bamford, G. Barentsen, P. Barmby, A. Baumbach, K. L. Berry, F. Biscani, M. Boquien, K. A. Bostroem, L. G. Bouma, G. B. Brammer, E. M. Bray, H. Breytenbach, H. Buddelmeijer, D. J. Burke, G. Calderone, J. L. Cano Rodríguez, M. Cara, J. V. M. Cardoso, S. Cheedella, Y. Copin, L. Corrales, D. Crichton, D. D'Avella, C. Deil, É. Depagne, J. P. Dietrich, A. Donath, M. Droettboom, N. Earl, T. Erben, S. Fabbro, L. A. Ferreira, T. Finethy, R. T. Fox, L. H. Garrison, S. L. J. Gibbons, D. A. Goldstein, R. Gommers, J. P. Greco, P. Greenfield, A. M. Groener, F. Grollier, A. Hagen, P. Hirst, D. Homeier, A. J. Horton, G. Hosseinzadeh, L. Hu, J. S. Hunkeler, Ž. Ivezić, A. Jain, T. Jenness, G. Kanarek, S. Kendrew, N. S. Kern, W. E. Kerzendorf, A. Khvalko, J. King, D. Kirkby, A. M. Kulkarni, A. Kumar, A. Lee, D. Lenz, S. P. Littlefair, Z. Ma, D. M. Macleod, M. Mastropietro, C. McCully, S. Montagnac, B. M. Morris, M. Mueller, S. J. Mumford, D. Muna, N. A. Murphy, S. Nelson, G. H. Nguyen, J. P. Ninan, M. Nöthe, S. Ogaz, S. Oh, J. K. Parejko, N. Parley, S. Pascual, R. Patil, A. A. Patil, A. L. Plunkett, J. X. Prochaska, T. Rastogi, V. Reddy Janga, J. Sabater, P. Sakurikar, M. Seifert, L. E. Sherbert, H. Sherwood-Taylor, A. Y. Shih, J. Sick, M. T. Silbiger, S. Singanamalla, L. P. Singer, P. H. Sladen, K. A. Sooley, S. Sornarajah, O. Streicher, P. Teuben, S. W. Thomas, G. R. Tremblay, J. E. H. Turner, V. Terrón, M. H. van Kerkwijk, A. de la Vega, L. L. Watkins, B. A. Weaver, J. B. Whitmore, J. Woillez, V. Zabalza, and (Astropy) Contributors. The Astropy Project: Building an Open-science Project and Status of the v2.0 Core Package. *AJ*, 156:123, September 2018. doi: 10.3847/1538-3881/aabc4f.

Adrian Price-Whelan. adrn/pyia: v0.2. Apr 2018. doi: 10.5281/zenodo.1228136.

L. M. Rebull, J. R. Stauffer, L. A. Hillenbrand, A. M. Cody, J. Bouvier, D. R. Soderblom, M. Pinsonneault, and L. Hebb. Rotation of Late-type Stars in Praesepe with K2. *ApJ*, 839:92, April 2017. doi: 10.3847/1538-4357/aa6aa4.

A. C. Robin, X. Luri, C. Reylé, Y. Isasi, E. Grux, S. Blanco-Cuaresma, F. Arenou, C. Babusiaux, M. Belcheva, R. Drimmel, C. Jordi, A. Krone-Martins, E. Masana, J. C. Mauduit, F. Mignard, N. Mowlavi, B. Rocca-Volmerange, P. Sartoretti, E. Slezak, and A. Sozzetti. Gaia Universe model snapshot. A statistical analysis of the expected contents of the Gaia catalogue. *A&A*, 543:A100, Jul 2012. doi: 10.1051/0004-6361/201118646.

E. Schatzman. A theory of the role of magnetic activity during star formation. *Annales d'Astrophysique*, 25:18, February 1962.

J. A. Sellwood. Secular evolution in disk galaxies. *Reviews of Modern Physics*, 86(1):1–46, Jan 2014. doi: 10.1103/RevModPhys.86.1.

A. Skumanich. Time Scales for CA II Emission Decay, Rotational Braking, and Lithium Depletion. *ApJ*, 171:565, February 1972. doi: 10.1086/151310.

F. Spada and A. C. Lanzafame. On the competing effect of wind braking and interior coupling in the rotational evolution of solar-like stars. *arXiv e-prints*, art. arXiv:1908.00345, Aug 2019.

Antony A. Stark and Jan Brand. Kinematics of Molecular Clouds. II. New Data on Nearby Giant Molecular Clouds. *ApJ*, 339:763, Apr 1989. doi: 10.1086/167334.

Antony A. Stark and Youngung Lee. The Scale Height of Giant Molecular Clouds Is Less than That of Smaller Clouds. *ApJ*, 619(2):L159–L162, Feb 2005. doi: 10.1086/427936.

J. L. van Saders, T. Ceillier, T. S. Metcalfe, V. Silva Aguirre, M. H. Pinsonneault, R. A. García, S. Mathur, and G. R. Davies. Weakened magnetic braking as the origin of anomalously rapid rotation in old field stars. *Nature*, 529:181–184, January 2016. doi: 10.1038/nature16168.

J. L. van Saders, M. H. Pinsonneault, and M. Barbieri. Forward Modeling of the Kepler Stellar Rotation Period Distribution: Interpreting Periods from Mixed and Biased Stellar Populations. *ArXiv e-prints*, March 2018.

E. J. Weber and L. Davis, Jr. The Angular Momentum of the Solar Wind. *ApJ*, 148:217–227, April 1967. doi: 10.1086/149138.

Andrew A. West, Dylan P. Morgan, John J. Bochanski, Jan Marie Andersen, Keaton J. Bell, Adam F. Kowalski, James R. A. Davenport, Suzanne L. Hawley, Sarah J. Schmidt, David Bernat, Eric J. Hilton, Philip Muirhead, Kevin R. Covey, Bárbara Rojas-Ayala, Everett Schlawin, Mary Gooding, Kyle Schluns, Saurav Dhital, J. Sebastian Pineda, and David O. Jones. The Sloan Digital Sky Survey Data Release 7 Spectroscopic M Dwarf Catalog. I. Data. *AJ*, 141(3):97, Mar 2011. doi: 10.1088/0004-6256/141/3/97.

This preprint was prepared with the AAS LaTeX macros v5.0.